Strength Prediction of Cruciform Specimen Under Biaxial Loading

Weng Jingmeng, *Wen Weidong* *, *Xu Ying*

Jiangsu Province Key Laboratory of Aerospace Power System, State Key Laboratory of Mechanics and Control of Mechanical Structures, Nanjing University of Aeronautics and Astronautics, Nanjing 210016, P. R. China

(Received 5 September 2016; revised 23 February 2017; accepted 3 May 2017)

Abstract: In order to achieve a better understanding of failure behavior of cruciform specimen under different biaxial loading conditions, a three-dimensional finite element model is established with solid and interface elements. Maximum stress criterion, two Hashin-type criteria and the new proposed criteria are used to predict the strength of plain woven textile composites when biaxial loading ratio equals 1. Compared with experimental data, only the new proposed criteria can reach reasonable results. The applicability of the new proposed criteria is also verified by predicting the tensile and compressive strength of cruciform specimen under different biaxial loading ratios. Moreover, the introduction of interface element makes it more intuitive to recognize delamination failure. The shape of the predicted delamination failure region in the interface layer is similar to that of the failure region in neighboring entity layers, but the area of delamination failure region is a little larger.

Key words: cruciform specimen; biaxial loading; progressive damage model; failure criteria; biaxial strength

CLC number: V231 **Document code**: A **Article ID**: 1005-1120(2017)03-0286-10

0 Introduction

Because of their outstanding mechanical properties, composite materials are widely used in aviation, aerospace, automotive and medicine field. The static strength and fatigue properties of composites under uniaxial loading are widely studied[1,2], while few experiments and finite element analysis have been conducted to investigate the behavior of composites under complex loading, like biaxial loading.

To generate a strength envelope in σ_1-σ_2 stress space, applying in-plane biaxial loads to cruciform specimen will be the most appropriate method[3]. Nevertheless, all researches have demonstrated that it is almost impossible to eliminate the stress concentration in the outer fillet corner between two perpendicular arms. Serna et al.[4,5] tested a chopped glass-reinforced composite from the experimental and numerical point of view, and the results showed that the crack emanates from the outer fillet corner between two perpendicular arms. In order to increase the likelihood of failure in the biaxially loaded test zone, it is necessary to reduce the thickness of the biaxially loaded test zone and optimize the corner geometry at the intersection between two perpendicular arms[3,6-9].

For cruciform specimen made of plain woven textile composites, Qian[6] studied the influence of various geometrical parameters by numerical simulation. Cruciform specimens with the optimal geometrical parameters were manufactured and tested under different biaxial loading conditions. Lin et al.[10] also studied the failure behavior of composite laminates for various layups and biaxial loading conditions by numerical investigation.

Under biaxial loading, the distribution and repartition of stress is not constant over the specimen. Therefore, strain field monitoring techniques are needed, such as strain gages or strain rosettes[6,7,11], high-speed stereo digital image correlation[12], infrared thermography[12,13], air-

* Corresponding author, E-mail address: gswwd@nuaa.edu.cn.

How to cite this article: Weng Jingmeng, Wen Weidong, Xu Ying. Strength prediction of cruciform specimen under biaxial loading[J]. Trans. Nanjing Univ. Aero. Astro., 2017,34(3):286-295.
http://dx.doi.org/10.16356/j.1005-1120.2017.03.286

coupled guided waves[13], and digital image correlation[3,14], etc.

Based on the strain field obtained experimentally, Lamkanfi et al.[15,16] compared three-dimensional finite element model with two-dimensional model. The results showed that strain distribution could only be modeled accurately by three-dimensional model. Delamination failure is one kind of damage forms between two layers. Different stress-based[17,18] and fracture-mechanics-based[19,20] failure criteria have been proposed. In Ref. [21], solid-shell interface element SOLSH190 was adopted to simulate the interface layer of laminated composites under impact load, the numerical results were in good agreement with experimental data.

The present paper focuses on characterizing the failure behavior of cruciform specimen under different biaxial loading conditions. First, referring to the cruciform specimen used in Ref. [6], a parametric three-dimensional finite element model is established in ANSYS platform, solid entity part and interface layer are both included in the finite element model. Subsequently, maximum stress criterion, criteria from Refs. [22—23], and the new proposed criteria are used to predict the strength of plain woven textile composites when biaxial loading ratio equals 1. The predicted results by different failure criteria are compared with experimental data. Then, the applicability of the new criteria is examined under different biaxial loading conditions. Finally, the progressive damage process of entity and interface layers of plain woven textile composites is analyzed in detail when biaxial loading ratio equals 1.

1 Experiment

For cruciform specimen made of plain woven textile composites, Qian[6] optimized the geometrical parameters of cruciform specimen by numerical simulation (Fig. 1). The values of the optimized dimension parameters are listed in Table 1. According to Fig. 1 and Table 1, 32 cruciform specimens were manufacrured with plain woven textile composites.

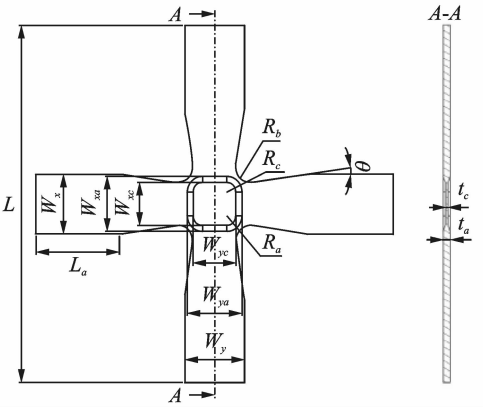

Fig. 1 Shape of cruciform specimen[6]

Table 1 Values of dimension parameters in Fig. 1

L/mm	W_x/mm	W_y/mm	L_a/mm	R_b/mm	W_a/mm
300	50	50	70	12	46
W_c/mm	R_a/mm	R_c/mm	t_a/mm	t_c/mm	θ/(°)
36	13	8	4.5	1.5	8

The tensile and compressive biaxial strength of cruciform specimens under four different biaxial loading ratios were tested, that is four tests for each biaxial loading condition. These cruciform specimens were biaxially loaded in its plane using SDS100. With four independent servo-hydraulic actuators and an appropriate control unit, SDS100 can keep the centre of the specimen at the same position during the loading process. Fig. 2 presents tensile failure form of cruciform specimen when biaxial loading ratio equals 1. The average values of tensile and compressive strength of cruciform specimens under different biaxial loading ratios are listed in Table 2.

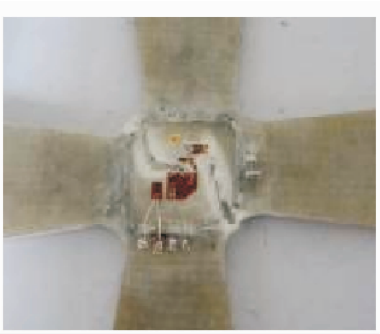

Fig. 2 Tensile failure form of cruciform specimen when biaxial loading ratio equals 1[6]

Table 2 Biaxial strength of cruciform specimens[6]

Biaxial loading ratio	Tensile strength/kN		Compressive strength/kN	
	Weft direction	Warp direction	Weft direction	Warp direction
1/1	19.95	19.99	14.28	14.25
1/2	20.96	10.47	14.87	7.45
1/3	21.72	7.24	15.92	5.35
1/4	22.42	5.61	16.28	4.07

2 Progressive Damage Model

A typical progressive damage model comprises three parts: Stress analysis, failure criteria and material property degradation rules. The progressive damage model of cruciform specimen under biaxial loading condition is developed by ANSYS parametric design language (APDL), the flow chart is plotted in Fig. 3.

Mechanical properties of composite materials are the basis of numerical simulation. The mechanical properties of plain woven textile composites and matrix in Tables 3, 4 are obtained from Ref. [6] and Ref. [24]. In Ref. [6], the material of strengthening plates are the same with experimental material.

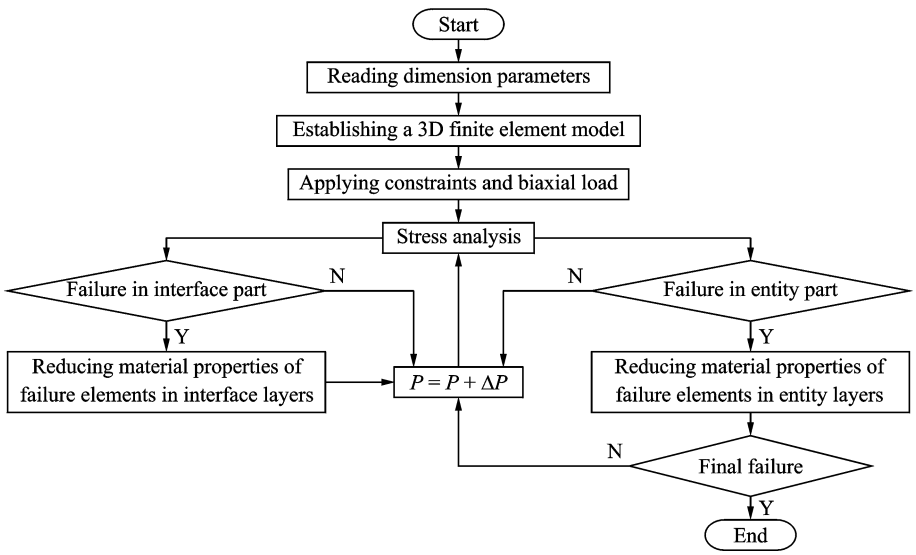

Fig. 3 Flow chart of predicting biaxial strength of cruciform specimen

Table 3 Mechanical properties of glass fiber-reinforced plain woven textile composites[6]

X_{1t}/MPa	X_{1c}/MPa	E_1/GPa	X_{2t}/MPa	X_{2c}/MPa	E_2/GPa	S_{12}/MPa	G_{12}/GPa	ν_{21}
385.42	279.36	21.5	385.42	279.36	21.5	68.45	3.42	0.11

Table 4 Mechanical properties of matrix[24]

X_{3t}/MPa	X_{3c}/MPa	E_3/GPa	ν_{21}	S_{12m}/MPa	G_{12m}/GPa
112	214	3.5	0.35	89.6	1.3

2.1 Stress analysis—finite element model

Referring to Fig. 1 and Table 1, a finite element model of cruciform specimen is established in ANSYS platform (Fig. 4). The finite element model is composed of 18 solid layers and 17 interface layers. Element SOLID45 is used to mesh the entity part of the cruciform specimen, and element SOLSH190 is used to simulate the interface between two layers.

According to Ref. [6], the cruciform specimen is with a central region of reduced thickness. The 1st—6th, the 12th—17th interface layers and the 1st—6th, the 13th—18th solid layers compose strengthening plates. The central zone of strengthening plates is subtracted according to Fig. 1. The biaxially loaded test zone in the finite element model is outlined in red on the right side of Fig. 4.

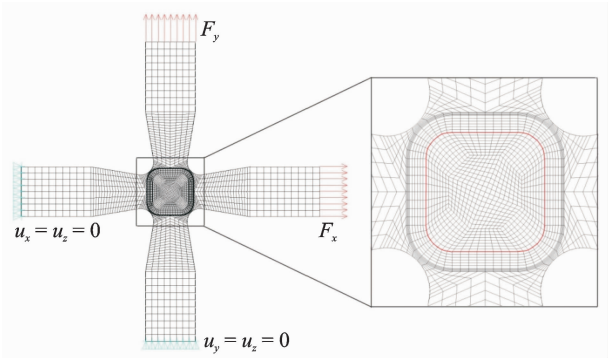

Fig. 4 Finite element model of cruciform specimen

2.2 Failure criteria

For plain woven textile composites, fiber tensile failure in weft and warp direction, fiber compressive failure in weft and warp directions, shear failure and delamination failure will occur during the load process. In order to predict all failure modes and biaxial strength, maximum stress criterion, criteria from Ref. [22] and Ref. [23] (Hashin-type criteria), and the new proposed criteria (Eqs. (1—8)) are used to predict the biaxial strength of plain woven textile composites.

2.2.1 Failure of entity layer

Fiber tensile failure in weft direction ($\sigma_{11}>0$)

$$\left(\cos\left|\frac{\sigma_{11}}{\sigma_{22}}\right|\right)\left(\frac{\sigma_{11}}{X_T}\right)^2+\alpha_{1T}\left(\frac{\dfrac{\tau_{12}^2}{2G_{12}}+\dfrac{3}{4}\alpha_S\tau_{12}^4}{\dfrac{S_{12}^2}{2G_{12}}+\dfrac{3}{4}\alpha_S S_{12}^4}\right)^2+\alpha_{1T}\left(\frac{\dfrac{\tau_{13}^2}{2G_{13}}+\dfrac{3}{4}\alpha_S\tau_{13}^4}{\dfrac{S_{13}^2}{2G_{13}}+\dfrac{3}{4}\alpha_S S_{13}^4}\right)^2\geqslant 1 \tag{1}$$

Fiber tensile failure in warp direction ($\sigma_{22}>0$)

$$\left(\cos\left|\frac{\sigma_{22}}{\sigma_{11}}\right|\right)\left(\frac{\sigma_{22}}{Y_T}\right)^2+\alpha_{2T}\left(\frac{\dfrac{\tau_{12}^2}{2G_{12}}+\dfrac{3}{4}\alpha_S\tau_{12}^4}{\dfrac{S_{12}^2}{2G_{12}}+\dfrac{3}{4}\alpha_S S_{12}^4}\right)^2+\alpha_{2T}\left(\frac{\dfrac{\tau_{23}^2}{2G_{23}}+\dfrac{3}{4}\alpha_S\tau_{23}^4}{\dfrac{S_{23}^2}{2G_{23}}+\dfrac{3}{4}\alpha_S S_{23}^4}\right)^2\geqslant 1 \tag{2}$$

Fiber compressive failure in weft direction ($\sigma_{11}<0$)

$$\left(\frac{\sigma_{11}}{X_C}\right)^2+\alpha_{1C}\left(\frac{\dfrac{\tau_{12}^2}{2G_{12}}+\dfrac{3}{4}\alpha_S\tau_{12}^4}{\dfrac{S_{12}^2}{2G_{12}}+\dfrac{3}{4}\alpha_S S_{12}^4}\right)^2+\alpha_{1C}\left(\frac{\dfrac{\tau_{13}^2}{2G_{13}}+\dfrac{3}{4}\alpha_S\tau_{13}^4}{\dfrac{S_{13}^2}{2G_{13}}+\dfrac{3}{4}\alpha_S S_{13}^4}\right)^2\geqslant 1 \tag{3}$$

Fiber compressive failure in warp direction ($\sigma_{22}<0$)

$$\left(\frac{\sigma_{22}}{Y_C}\right)^2+\alpha_{2C}\left(\frac{\dfrac{\tau_{12}^2}{2G_{12}}+\dfrac{3}{4}\alpha_S\tau_{12}^4}{\dfrac{S_{12}^2}{2G_{12}}+\dfrac{3}{4}\alpha_S S_{12}^4}\right)^2+\alpha_{2C}\left(\frac{\dfrac{\tau_{23}^2}{2G_{23}}+\dfrac{3}{4}\alpha_S\tau_{23}^4}{\dfrac{S_{23}^2}{2G_{23}}+\dfrac{3}{4}\alpha_S S_{23}^4}\right)^2\geqslant 1 \tag{4}$$

Shear failure in weft direction

$$\alpha_{1s}\left(\frac{\dfrac{\tau_{12}^2}{2G_{12}}+\dfrac{3}{4}\alpha_S\tau_{12}^4}{\dfrac{S_{12}^2}{2G_{12}}+\dfrac{3}{4}\alpha_S S_{12}^4}\right)^2+\alpha_{2s}\left(\frac{\dfrac{\tau_{13}^2}{2G_{13}}+\dfrac{3}{4}\alpha_S\tau_{13}^4}{\dfrac{S_{13}^2}{2G_{13}}+\dfrac{3}{4}\alpha_S S_{13}^4}\right)^2\geqslant 1 \tag{5}$$

Shear failure in warp direction

$$\alpha_{1s}\left(\frac{\dfrac{\tau_{12}^2}{2G_{12}}+\dfrac{3}{4}\alpha_S\tau_{12}^4}{\dfrac{S_{12}^2}{2G_{12}}+\dfrac{3}{4}\alpha_S S_{12}^4}\right)^2+\alpha_{2s}\left(\frac{\dfrac{\tau_{23}^2}{2G_{23}}+\dfrac{3}{4}\alpha_S\tau_{23}^4}{\dfrac{S_{23}^2}{2G_{23}}+\dfrac{3}{4}\alpha_S S_{23}^4}\right)^2\geqslant 1 \tag{6}$$

In Eqs. (1)—(6), σ_{ij} ($i,j=1,2,3$) are the stress components, X_T, X_C, Y_T, Y_C the tensile and the compressive strength of composites in the weft and the warp directions, respectively; S_{ij}, G_{ij} ($i,j=1,2,3$) the shear strength and the modulus of composites in corresponding directions; α_s is the material nonlinear factor; and α_{1T}, α_{1C}, α_{2T}, α_{2C}, α_{1S}, α_{2S} are the shear contribution factors in each failure mode.

2.2.2 Failure of interface layer

Most stress-based delamination failure criteria[17,25] determine whether delamination is initiated according to the stress field and strength in layer. This is not very precise. For instance, all the 21 plies of composite plates have delamination failure in Ref. [17] (Fig. 5), but there are only 20 interfaces actually, i. e., the number of delaminated layers is not equal to the number of inter-

faces. Therefore, the introduction of interface layer in numerical simulation is necessary.

Fig. 5 Predicted delamination after impact[17]

In reality, tensile stress and compressive stress can both cause delamination failure. Since the material properties of interface layer are set the same with matrix, the new proposed delamination criteria for tensile stress and compressive stress are formulated as Eq. (7) and Eq. (8), respectively.

With the introduction of interface layer, the delamination failure criterion of maximum stress criterion and criteria from Refs. [22,23] are modified to the delamination failure criterion developed in this paper (Eqs. (7,8)), while fiber failure criterion and shear failure criterion remain unchanged as the original.

Tensile delamination failure ($\sigma_{11}+\sigma_{22}+\sigma_{33}>0$)

$$\left(\frac{\sigma_{11}+\sigma_{22}+\sigma_{33}}{X_{\mathrm{TM}}}\right)^2+\frac{\tau_{12}^2}{S_{12\mathrm{m}}^2}+\frac{\tau_{13}^2}{S_{13\mathrm{m}}^2}+\frac{\tau_{23}^2}{S_{23\mathrm{m}}^2}\geqslant 1 \tag{7}$$

Compressive delamination failure ($\sigma_{11}+\sigma_{22}+\sigma_{33}<0$)

$$\left(\frac{\sigma_{11}+\sigma_{22}+\sigma_{33}}{X_{\mathrm{CM}}}\right)^2+\frac{\tau_{12}^2}{S_{12\mathrm{m}}^2}+\frac{\tau_{13}^2}{S_{13\mathrm{m}}^2}+\frac{\tau_{23}^2}{S_{23\mathrm{m}}^2}\geqslant 1 \tag{8}$$

where X_{TM}, X_{CM} are the tensile and the compressive strength of matrix, $S_{ij\mathrm{m}}$ $(i,j=1,2,3)$ the shear strength of matrix.

2.3 Material property degradation rules

In order to evaluate the applicability of different failure criteria for plain woven textile composites, only one kind of material property degradation rules is adopted. The reduction factors of failure in entity part of composites are the same as Ref. [22]. In Ref. [22], delamination failure is predicted by the stress field and strength in layer, i. e., interface element is not included. Therefore, the material property degradation rule corresponding to delamination failure is not suitable for this paper. The reduction factor of failure in interface layer of composites is stipulated as follows.

(1) Fiber tensile failure in weft direction: E_1, G_{12}, G_{13}, ν_{12}, ν_{13} are degraded to 0.16 of their initial values;

(2) Fiber compressive failure in weft direction: E_1, G_{12}, G_{13}, ν_{12}, ν_{13} are degraded to 0.32 of their initial values;

(3) Fiber tensile failure in warp direction: E_2, G_{12}, G_{23}, ν_{12}, ν_{23} are degraded to 0.16 of their initial values;

(4) Fiber compressive failure in warp direction: E_2, G_{12}, G_{23}, ν_{12}, ν_{23} are degraded to 0.32 of their initial values;

(5) Shear failure in weft and warp direction: G_{12} and ν_{12} are degraded to 1×10^{-6} of their initial values;

(6) Interface failure: All material properties are degraded to 1×10^{-6} of their initial values.

3 Results and Discussion

By using the progressive damage model, the whole process of damage propagation and failure strength of glass fiber-reinforced plain woven textile composites under different biaxial loading ratios are studied.

3.1 Comparison of failure criteria

Maximum stress criterion, criteria from Ref. [22], criteria from Ref. [23] and the new proposed criteria are used to predict the strength of plain woven textile composites when biaxial loading ratio equals 1.

In maximum stress criterion, fiber failure occurs if the principal stress is greater than the corresponding strength in each material principal direction. In criteria from Refs. [22,23], fiber failure occurs when a determined quadratic inequality of stress components is satisfied. The criteria used in Ref. [22] take three-dimensional stress tensor into consideration. While criteria used in

Ref. [23] take two-dimensional stress tensor into account. However, all the shear contribution factors in these two criteria are equal to 1.

From Table 5, it is observed that maximum stress criterion overestimates the biaxial strength of cruciform specimen. Criteria from Refs. [22, 23] underestimate the biaxial strength. Using the new proposed criteria, the relative errors between the predicted results and the experimental ones are within 5%.

Since the material of each layer is plain woven textile composites, the damage of each layer in the biaxially loaded test zone is almost the same. So only the first entity ply is given in Fig. 6. The red and the blue elements denote that fiber tensile failure occurs in weft and warp directions, respectively. The orange element denotes that fiber tensile failure occurs in weft and warp directions simultaneously. In the process of progressive damage analysis, when fiber tensile/compressive failure elements divide the cruciform specimen into two parts, the corresponding strength is stipulated as the final failure strength.

From Fig. 6, it is clear that when using the criteria from Ref. [23], final failure occurs outside the biaxially loaded test zone, and there is no any damage in the central region. When using the criteria from Ref. [22], fiber failure in weft or/and warp directions occurs in the biaxially loaded test zone, but the very central region is undamaged. From Figs. 6(b,e), the failure modes predicted by maximum stress criterion and the criteria proposed in this paper are consistent with the fracture path of the specimen (Fig. 2). Combined with the predicted tensile failure strength, the new criteria is the only one which predicts the biaxial strength of plain woven textile composites reasonably.

Table 5 Comparison of failure criteria (biaxial loading ratio equals 1)

Criteria	Weft direction		Warp direction	
	Failure strength/kN	Error/%	Failure strength/kN	Error/%
Experimental value[6]	19.95		19.99	
Maximum stress criterion	24.612 50	23.37	24.612 50	23.12
Criteria from Ref. [22]	12.306 25	−38.31	12.306 25	−38.44
Criteria from Ref. [23]	14.543 75	−27.10	14.543 75	−27.24
The new criteria	19.018 75	−4.67	19.018 75	−4.86

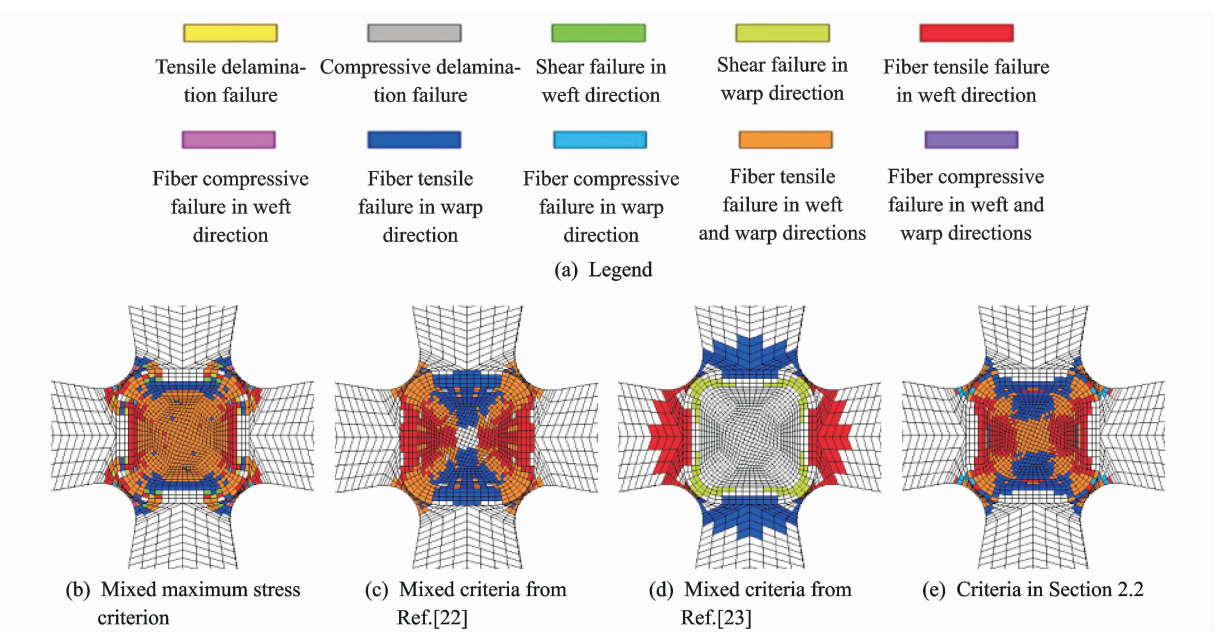

Fig. 6 Final failure of cruciform specimens

3.2 Verification for different biaxial loading ratios

In order to verify the applicability of the new proposed criteria, the biaxial tensile and compressive strength of plain woven textile composites under different biaxial loading ratios are predicted. The comparison of predicted results and experimental ones are shown in Table 6. It can be seen that the relative errors of the predicted strength are within 10%.

Table 6 Comparison of biaxial failure strength

Biaxial loading ratio		Weft direction			Warp direction		
		Experimental value/kN	Predicted value/kN	Error/%	Experimental value/kN	Predicted value/kN	Error/%
Tensile strength	1/1	19.95	19.018 75	−4.67	19.99	19.018 75	−4.86
	1/2	21.72	22.375 00	6.75	10.47	11.187 50	6.85
	1/3	21.72	23.493 75	8.17	7.24	7.831 25	8.175
	1/4	22.42	22.375 00	−0.20	5.61	5.593 75	0.29
Compressive strength	1/1	14.28	13.425 00	−5.99	14.25	13.425 00	−5.79
	1/2	14.87	15.662 50	5.33	7.45	7.831 25	5.12
	1/3	15.92	16.781 25	5.41	5.35	5.593 75	4.56
	1/4	16.28	17.900 00	9.95	4.07	4.475 00	9.95

3.3 Progressive damage process

When biaxial loading ratio equals 1, the initial and final failure of the cruciform specimen under biaxial tensile loading is shown in Fig. 7.

When $F_x = F_y = 17.9$ kN, tensile delamination failure occurs firstly in the inner fillet corners of the 6th and 12th interface layers (Fig. 7(b)). The 6th and 12th interface layers are the two layers which lie between the strengthening plates and the test specimen.

As the biaxial tensile load increases, the damage grows gradually. The final failure of cruciform specimen occurs when $F_x = F_y = 19.018\ 75$ kN. Due to the symmetry of the structure, only the 1st—9th entity layers and interface layers are plotted in Fig. 7(c). It can be seen that, in each entity layer of the strengthening plates, fiber tensile failure in weft and warp directions (orange elements) occurs in the connection region between two perpendicular arms.

In the biaxially loaded test zone of the 7th—9th entity layers, the orange elements present an "X". This is because the original material me-

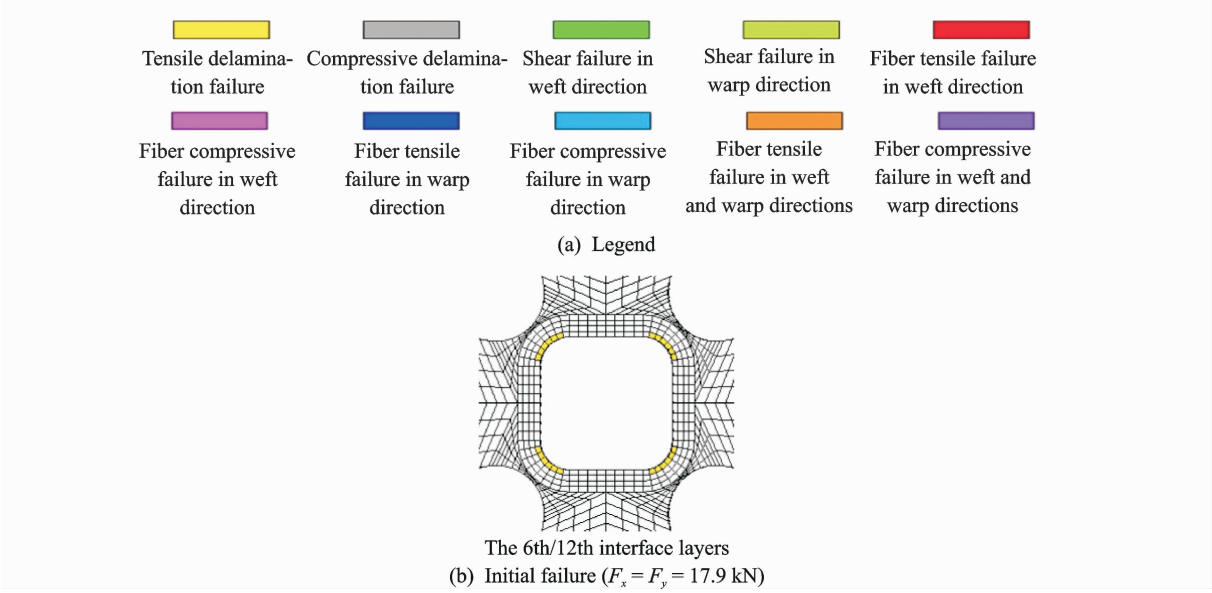

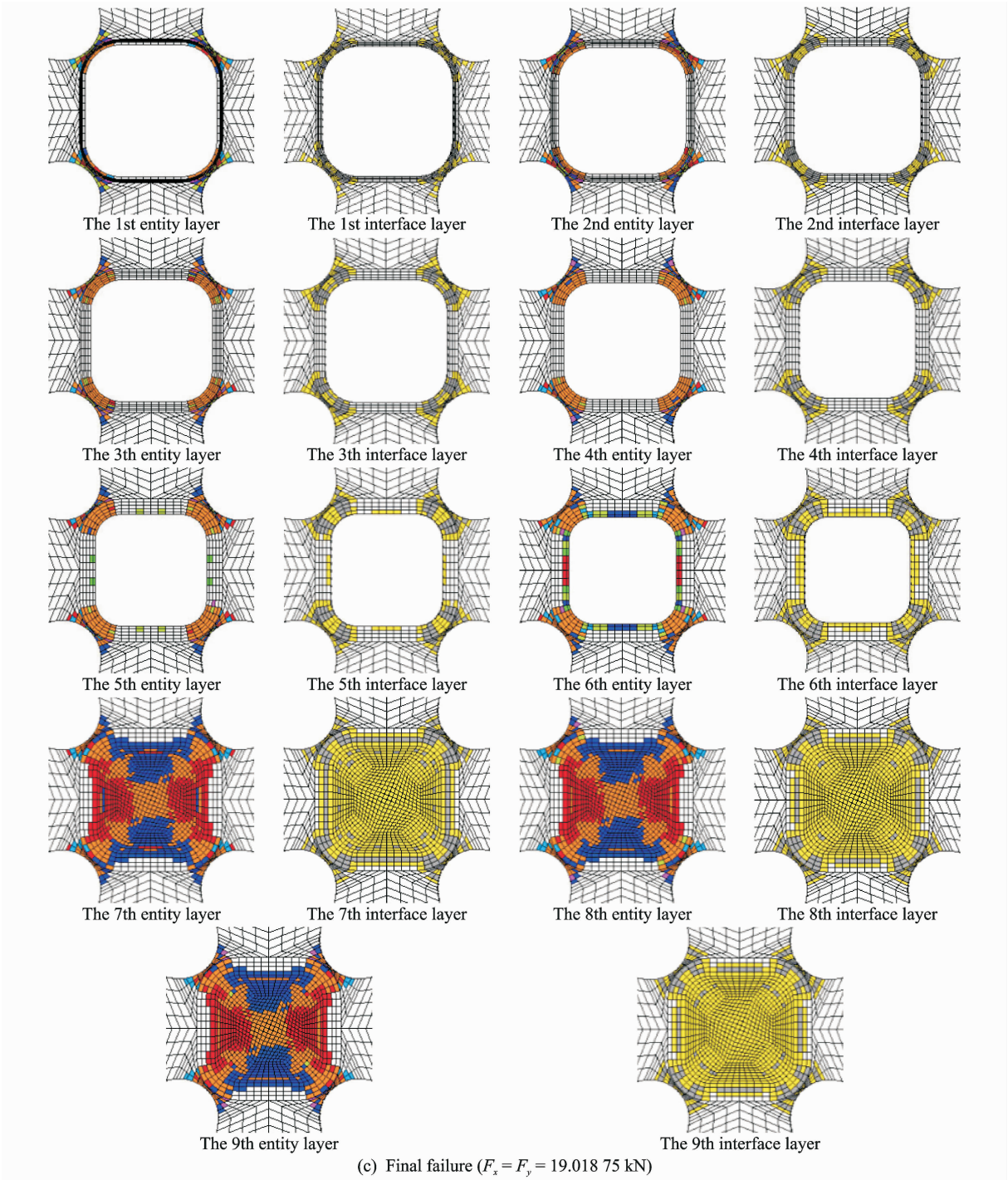

(c) Final failure ($F_x = F_y = 19.018\ 75$ kN)

Fig. 7 Progressive damage process under biaxial tensile loading ($\sigma_1/\sigma_2 = 1$)

chanical properties of each element in the finite element model are the same with each other, while the material mechanical properties of real specimen are non-identical on account of defects. The crack will occur and propagate in the weakest region of the specimen. Therefore, in the finite element model, the region of orange elements gives the most probable area where the fracture path of the specimen may occur. In the interface layers, it can be seen that there are few compressive delamination failure elements near the fillet corners, but only tensile delamination failure occurs in the biaxially loaded test zone. Besides, the shape of delamination failure in each interface layer is similar to that of failure region in neighboring entity layer, but the area of delamination

failure region is a little larger, which agrees well with experimental results.

4 Conclusions

The damage evolution of cruciform specimen is analyzed by progressive damage model, and the biaxial strength of plain woven textile composites is predicted. Some conclusions can be obtained as follows:

(1) When biaxial loading ratio equals 1, the maximum stress criterion overestimates the strength of cruciform specimen, while the criteria from Refs. [22,23] underestimate the strength. When using the new proposed criteria in this paper, the relative errors between the predicted results and the experimental ones are within 5%. In addition, the new criteria give the most suitable fracture path for cruciform specimen.

(2) The new proposed criteria are verified by predicting the biaxial tensile and compressive strength of cruciform specimen under different biaxial loading ratios. The numerical results agree well with experimental data.

(3) The introduction of interface element makes it more intuitive to recognize delamination failure. In the tensile process, delamination failure occurs firstly in the fillet corners of the interface layers which lie between the strengthening plates and the test specimen. With the load increasing, delamination failure grows gradually. The shape of delamination failure in each interface layer is similar to that of failure region in neighboring entity layer, but the area of delamination failure region is a little larger.

Acknowledgments

This work was supported by the National Natural Science Foundation of China (No. 51205190) and the Jiangsu Province Key Laboratory of Aerospace Power System (No. NJ20140019).

References:

[1] HUAN Dajun, DING Bing, LI Yong, et al. High velocity impact experiment on Ti/CFRP/Ti sandwich structure[J]. Trans. Nanjing Univ. Aero. Astro., 2015, 32(1): 121-127.

[2] ZHOU Guangming, WANG Ning. Numerical analysis and test evaluation on cryogenic mechanical properties of two-dimensional woven composite[J]. Journal of Nanjing University of Aeronautics & Astronautics, 2014, 46(6): 838-844. (in Chinese)

[3] SMITS A, van HEMELRIJCK D, PHILIPPIDIS T P, et al. Design of a cruciform specimen for biaxial testing of fibre reinforced composite laminates[J]. Composites Science and Technology, 2006, 66(718): 964-975.

[4] SERNA M M C, CURIEL-SOSA J L, NAVARRO-ZAFRA J, et al. Crack propagation in a chopped glass-reinforced composite under biaxial testing by means of XFEM[J]. Composite Structures, 2015, 119: 264-271.

[5] SERNA M M C, MARTÍNEZ V J L, LÓPEZ C J J. Failure strain and stress fields of a chopped glass-reinforced polyester under biaxial loading[J]. Composite Structures, 2013, 103: 27-33.

[6] QIAN Yuan. Structure design and experimental investigation of burst composites canister cover[D]. Nanjing: Nanjing University of Aeronautics and Astronautics, 2013. (in Chinese)

[7] LU Xiaohua. Strength criteria investigation and biaxial tensile experimental of 2-axial fiber-reinforced composites[D]. Nanjing: Nanjing University of Aeronautics and Astronautics, 2007. (in Chinese)

[8] MAKRIS A, VANDENBERGH T, RAMAULT C, et al. Shape optimisation of a biaxially loaded cruciform specimen[J]. Polymer Testing, 2010, 29(2): 216-223.

[9] WELSH J S, ADAMS D F. An experimental investigation of the biaxial strength of IM6/3501-6 carbon/epoxy cross-ply laminates using cruciform specimens [J]. Composites Part A-Applied Science and Manufacturing, 2002, 33(6): 829-839.

[10] LIN W P, HU H T. Parametric study on the failure of fiber-reinforced composite laminates under biaxial tensile load[J]. Journal of Composite Materials, 2002, 36(12): 1481-1503.

[11] SUN X S, HARIS A, TAN V B C, et al. A multiaxial fatigue model for fiber-reinforced composite laminates based on Puck's criterion[J]. Journal of Composite Materials, 2012, 46(4): 449-469.

[12] BUSCA D, FAZZINI M, LORRAIN B, et al. High-speed stereo digital image correlation: Application to biaxial fatigue[J]. Strain, 2014, 50(5): 417-427.

[13] RHEINFURTH M, SCHMIDT F, DÖRING D,

et al. Air-coupled guided waves combined with thermography for monitoring fatigue in biaxially loaded composite tubes[J]. Composites Science and Technology, 2011, 71(5): 600-608.

[14] LECOMPTE D, SMITS A, SOL H, et al. Mixed numerical-experimental technique for orthotropic parameter identification using biaxial tensile tests on cruciform specimens[J]. International Journal of Solids and Structures, 2007, 44(5): 1643-1656.

[15] LAMKANFI E, van PAEPEGEM W, DEGRIECK J, et al. Strain distribution in cruciform specimens subjected to biaxial loading conditions. Part 2: Influence of geometrical discontinuities[J]. Polymer Testing, 2010, 29(1): 132-138.

[16] LAMKANFI E, van PAEPEGEM W, DEGRIECK J, et al. Strain distribution in cruciform specimens subjected to biaxial loading conditions. Part 1: Two-dimensional versus three-dimensional finite element model[J]. Polymer Testing, 2010, 29(1): 7-13.

[17] HOU J P, PETRINIC N, RUIZ C, et al. Prediction of impact damage in composite plates[J]. Composites Science and Technology, 2000, 60(2): 273-281.

[18] TSERPES K I, LABEAS G, PAPANIKOS P, et al. Strength prediction of bolted joints in graphite/epoxy composite laminates[J]. Composites Part B: Engineering, 2002, 33(7): 521-529.

[19] WANG W, WAN X, ZHOU J, et al. Damage and failure of laminated carbon-fiber-reinforced composite under low-velocity impact[J]. Journal of Aerospace Engineering, 2014, 27(2): 308-317.

[20] SHI Y, PINNA C, SOUTIS C. Modelling impact damage in composite laminates: A simulation of intra- and inter-laminar cracking[J]. Composite Structures, 2014, 114: 10-19.

[21] ZHANG Haibo. A new 3D interface element for delamination simulation of laminated plates[D]. Tianjin: Tianjin University, 2009. (in Chinese)

[22] ZHU Zhenzhen. Research on prediction of fatigue life for woven composite laminate with hole[D]. Nanjing: Nanjing University of Aeronautics and Astronautics, 2010. (in Chinese)

[23] XIAO J R, GAMA B A, GILLESPIE J W. Progressive damage and delamination in plain weave S-2 glass/SC-15 composites under quasi-static punch-shear loading[J]. Composite Structures, 2007, 78(2): 182-196.

[24] TANG Jieyao. Research on inter-layer performance of 2.5D woven composites[D]. Nanjing: Nanjing University of Aeronautics and Astronautics, 2013. (in Chinese)

[25] BREWER J C, Lagace P A. Quadratic stress criterion for initiation of delamination[J]. Journal of Composite Materials, 1988, 22(12): 1141-1155.

Ms. **Weng Jingmeng** is a Ph. D. candidate in the College of Energy and Power Engineering at Nanjing University of Aeronautics and Astronautics. Her area of research is static strength and fatigue behaviors of composite materials.

Prof. **Wen Weidong** is Ph. D. advisor at Nanjing University of Aeronautics and Astronautics. His main research interests are strength and fatigue behaviors of advanced composite materials, strength and vibration of aviation power structures, etc.

Ms. **Xu Ying** is an associate professor and master tutor at Nanjing University of Aeronautics and Astronautics. Her main research interests are strength and fatigue behaviors of advanced composite materials, physical design method of advanced structures, etc.

(Executive Editor: Zhang Bei)